Reduction of Dispersion in Ultrasonically-Enhanced Micropacked Beds

Reduction of Dispersion in Ultrasonically-Enhanced Micropacked Beds

Francisco J. Navarro-Brull[1,2], Andrew R. Teixeira[2,3], Jisong Zhang[2], Roberto Gómez[1], Klavs F. Jensen[2*]

[1] Institut Universitari d'Electroquímica i Departament de Química Física, Universitat d'Alacant, Apartat 99, E-03080, Alicante, Spain

[2] Department of Chemical Engineering, Massachusetts Institute of Technology, Cambridge, MA 02139, United States

[3] Department of Chemical Engineering, Worcester Polytechnic Institute, Worcester, MA 01609, United States

Keywords: microreactor, channeling, capillary fingering, ultrasound, fluidization, sonochemistry, multiphase, hydrodynamics

ABSTRACT: Channeling of gas can reduce mass transfer performance in multiphase micropacked-bed reactors. Viscous and capillary forces cause this undesired and often unpredictable phenomenon in systems with catalyst particle sizes of hundreds of microns. In this work, we acoustically modify flow in a micropacked-bed reactor to reduce gas channeling by applying high-power sonication at low ultrasonic

frequencies (~40 kHz). Experimental residence time distributions reveal two orders of magnitude reduction in dispersion with ultrasound, allowing for nearly plug-flow behavior at high flow rates in the bed. Sonication appears to partially fluidize the packed-bed under pressurized co-current two-phase flow, effectively improving dispersion characteristics.

1. INTRODUCTION

The use of micropacked-bed reactors for multiphase catalyst testing has been limited by their complex and poorly understood hydrodynamics[1–5]. Capillary forces increase as the particle size decreases to hundreds of microns. The benefits provided by the increase of catalytic surface area and liquid hold-up (~75%) are counteracted by the formation of gas preferential channels, which significantly reduces gas-liquid interaction[6]. The unpredictable nature of gas-channeling phenomena is directly linked to the randomly-packed skeleton of particles within the bed. Furthermore, wall-effects tend to channel the gas phase preferentially to flow near the wall due to the inevitable local increase in porosity[7]. Consequently, poor radial-mass-transfer coefficients are achieved, especially when the reactor diameter increases[4]. Unfortunately, increasing gas and liquid flow rates cannot eliminate these strong and stable gas-channels produced by capillary forces[4]. Consequently, there is a lack of reliable dispersion and mass-transfer expressions[8] when designing packed-bed reactors with particle diameter below 500 μm.

In related studies of fluid-fluid multiphase flows through small porous domains (e.g., oil recovery and reservoirs, geological carbon dioxide sequestration) preferential flow channels are usually classified as capillary or viscous fingering[9]. The capillary number ($Ca \cong \mu v/\gamma$) discerns what kind of fingering can occur, where γ is the surface tension, μ the viscosity and v the velocity of the fluid being displaced. Interestingly, for capillary flow regimes ($Ca \ll 1$), reducing the surface wettability of the particles can help to reduce flow maldistribution to some extent[10,11]. On the other hand, the effect of geometric disorder can promote viscous fingering[12] even at relatively low capillary numbers ($Ca \sim 10^{-2}$). Under

these relatively similar and limiting circumstances, application of low frequency acoustic excitations during drainage promotes rapid pore-scale fluid invasions (also called bursts or Haines jumps) reducing air-entry capillary pressure in unsaturated soils[13]. Transient stress is known to produce an increase of permeability[14,15] and wave induced fluid flow[16]. Vibration-induced particle motion by using audible frequencies (50 and 500 Hz) has also been reported for unconsolidated media with liquid and dispersed gas bubbles[17,18]. In oil-recovery systems, where unfavorable viscous conditions exist, ultrasound irradiation has been successfully used to modify the porous structure showing 10% to 50% enhancement in permeation[19,20]. Within this context the use of acoustic energy in multiphase porous media can be an interesting approach to counteract gas-channeling mass-transfer limitations in micropacked-bed reactors for catalysis.

Acoustically generated cavitation has been widely used to enhance mass transfer in multiphase systems or even to induce unique *sono*-chemical reactions[21,22]. Ultrasound is typically applied in two ways: via ultrasonic baths[23] (indirect transmission of acoustic power) or by directly contacting the medium with ultrasonic horns or transducers [24–26]. Although the former has operational advantages such as its simplicity, using water as a transmission medium incurs a loss of acoustic power because of impedance mismatch and cavitation on the exterior reactor walls. By contrast, direct sonication efficiently affects the medium, although temperature control becomes crucial due to mechanically induced heat gains. To this end, Langevin-type transducers (also known as half-wave or sandwich transducers) provide high electro-acoustical efficiency and relatively-low heat generation[27]. To minimize sound attenuation counter-effects where the applied energy is transformed into heat, ultrasound applications are usually operated in the low-frequency region (20-80 kHz). These conditions involving high-energy conversion at low ultrasound frequency ranges are known in the literature as power ultrasound[27]. The proper design of power ultrasound equipment such ultrasonic horns or ultrasonic cleaning transducers usually involves the use of finite element analysis[28,29]. The general idea is to design

a resonant structure that vibrates orthogonal to the target forming standing waves with maximum amplitude at the extremes of the device[27]. The final shape of these half-wavelength resonators is designed to match acoustic impedances and maximize the amplitude within the mechanical limits of the construction material[30]. For example[27], radiation surfaces of tapered probes in ultrasonic horns can achieve power densities within the order of several hundred W/cm^2. The surface of sandwiched transducers, as used in ultrasonic baths and other applications, range in the order of 1-2 W/cm^2.

In this work, ultrasound irradiation is shown to reduce dispersion in micropacked bed reactors at high liquid and gas flow rates. Specifically, a reactor sonotrode is designed to mitigate gas-channeling phenomena with a resulting two orders of magnitude reduction of the liquid dispersion within the micropacked-bed.

2. METHODS

US-Reactor Design

The acoustic design of chemical reactors is not well established. The proper design of a reactor sonotrode is extremely sensitive to the operating frequency of interest, construction material(s), assembly, and geometry. As a consequence, several considerations were necessary to guarantee the correct transmission of acoustic power into the reactor medium. We followed the following steps to avoid the iterative experimental trial and error: i) frequency and transducer selection; ii) analytic dimensioning; iii) numerical modeling and design; and iv) final frequency tuning. The micropacked-bed sonotrode system resonated at 38.0 kHz consuming a maximum of 20 W of load power (Figure 1b). The horizontal stepped design provided sufficient displacement gains as illustrated in darker colors. The simulation results were obtained using our previously described model[29], using Biot's equations to capture the propagation of ultrasound within the porous bed medium[31,32]. Additional details can be found in the Supporting Information and elsewhere[28,29,33].

Ultrasonic systems require temperature control[34] since they are susceptible to erroneous measurements induced by thermal-fluctuations. For example, localized heat gains result from mechanical vibrations at solid-solid interfaces (friction), non-isothermal deformations (dampening) and cavitation. These thermal gradients can artificially increase the temperature within the packed bed masking effects of interest, including fluidization or gas-channeling reduction. Temperature control was achieved by combining forced air cooling over the transducer with an agitated water bath to provide/remove heat from the reactor sonotrode made of aluminum. Additional consideration was given to the options of: a) operating at elevated temperatures (60 - 70°C) with external heat addition by a proportional-integral-derivative (PID) controller, b) operating at lower total power, c) operating in 'burst' mode[27] whereby pulsed or modulated sonication power is supplied (commonly, 0.5 s bursts of power in cycles of 1 s).

RTD Experimentation Setup

To accurately measure the dispersion and liquid holdup in the multiphase system, a modified version of a residence time distribution apparatus[35–37] was used (Figure 1a). The micropacked-bed sonoreactor had a length of 100 mm and inner-outer diameters of 3.175 and 6.35 mm, respectively. Stainless steel beads of diameter 0.2 mm were used to pack the bed, and both water and nitrogen were fed continuously into the system at flow rates of 1-5 $mL \cdot min^{-1}$ and 10-20 sccm, respectively. Bed porosity, determined by weight, was 0.37. No statistical difference was observed between the particle size distribution of fresh and sonicated packing materials. The entire setup (see SI) was automated for reproducible measurement environments and data acquisition. Repeated tracer-response curves were combined and deconvoluted to obtain highly reproducible quantitative dispersion and residence time data. Erioglaucine (Brilliant Blue FCF) was purchased from spectrum chemical MFG Corp and used as a tracer in all RTD studies.

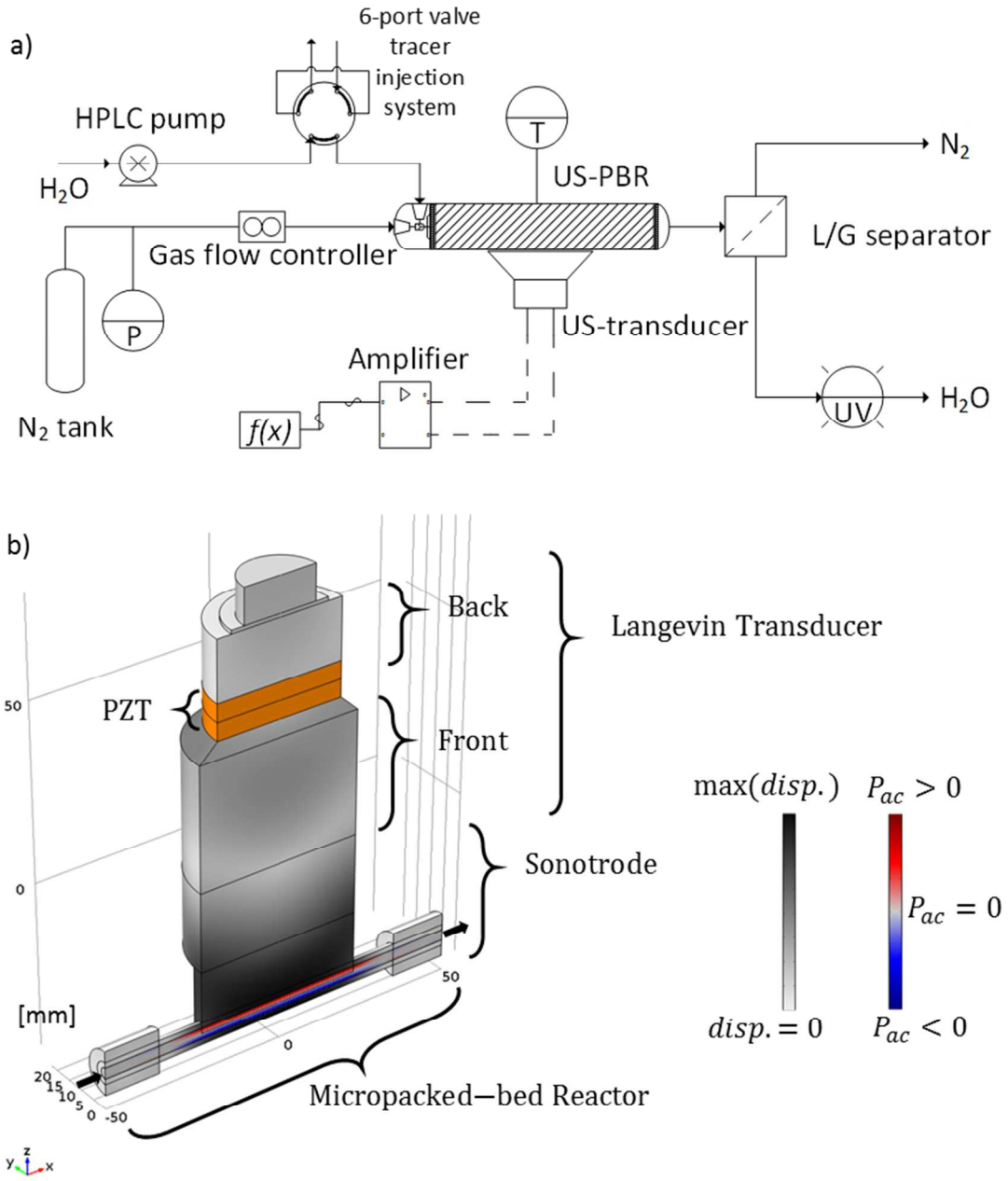

Figure 1. Automated micropacked-bed reactor platform with ultrasound assisted dispersion, RTD flow configuration shown (a). A commercial ultrasonic transducer (APC International, Ltd.) is tightly bolted to the acoustically designed (one-piece) sonotrode that resonates at c.a. 38 kHz (b). The assembled micropacked-bed sonoreactor enables the efficient transmission of acoustic power into the reactor

chamber. The red-blue color code indicates positive and negative acoustic pressure, whereas gray scale indicates the displacement of solid materials; orange disks define the piezoelectric transducer.

Given the sonoreactor dimensions and operating conditions, it is possible to analyze the relative strength of the different forces involved (Table 1) in order to verify hydrodynamic differences when compared with larger-scale trickle-bed reactors. As expected in micropacked-bed systems, inertial and gravitational forces have little to no effect on the hydrodynamics. The reduced particle diameter will generate narrow restrictions that increase the capillary forces even at moderately high liquid and gas flow rates. This will cause the gas to have a stronger tendency to continuously flow (rather than shear to form bubbles), hence the formation of preferential channels as the liquid permeates through most of the porous skeleton. However, sound propagation in the porous media benefits from the resultant higher liquid content in the bed —ranging from 0.65 to 0.85 liquid hold-up—in contrast to larger scale trickle-bed reactors with particle size ranging 1-3 mm.

Table 1. Dimensionless analysis[8] to characterize multiphase flow in packed-bed reactors

$\text{Reynolds}\ (Re_p)$	$=$	$\frac{\text{inertial force}}{\text{viscous force}}$	$=$	$\frac{\rho_L \mathbf{u}_{\text{s,L}} d_p}{\mu_L}$	$\approx$	2	Eq. 1
$\text{Capillary}\ (Ca_L)$	$=$	$\frac{\text{viscous force}}{\text{capillary force}}$	$=$	$\frac{\mu_L \mathbf{u}_{\text{s,L}}}{\gamma}$	$\approx$	$1.5 \cdot 10^{-4}$	Eq. 2
$\text{Bond}\ (Bo) = \text{Eötvös}\ (Eo)$	$=$	$\frac{\text{gravitational force}}{\text{capillary force}}$	$=$	$\frac{(\rho_L - \rho_G) g d_p^2}{\gamma}$	$\approx$	$5 \cdot 10^{-3}$	Eq. 3
$\text{Weber}\ (We)$	$=$	$\frac{\text{inertial force}}{\text{capillary force}}$	$=$	$\frac{\rho_L \mathbf{u}_{\text{s,L}}^2 d_p}{\gamma}$	$\approx$	$1 \cdot 10^{-4}$	Eq. 4

An additional setup was used in order to directly visualize the effects of power ultrasound in the fluid dynamics of co-current flow. Specifically, a titanium probe (diameter = 6.35 mm) of an ultrasonic horn was introduced concentrically into a micropacked-bed reactor (glass cylinder) of 9.525 mm ID containing glass-beads of diameter 100 μm. Imaging (30 fps) was performed on the system under well-developed

gas-liquid flow in the absence of ultrasound and with a steady addition of acoustic energy. Transient and steady profiles were captured in both the sonicated and silent portions of the bed. The recorded images were stabilized and adjusted using Adobe Premiere and analyzed using the Time-Resolved Digital Particle Image Velocimetry Tool[38] for MATLAB. More details regarding the experimental setup and image processing can be found in the SI.

Residence time distributions

In order to describe the non-ideal behavior of the liquid residence time distributions (RTDs), an axial dispersion model was used[39]:

$$\frac{\partial c}{\partial t} + \nabla \cdot (-D_a \nabla c + \mathbf{u}c) = 0 \qquad \text{Eq. 5}$$

where c [kmol·m^{-3}] is the concentration of the tracer, t [s] is the time, D_a [m^2·s^{-1}] is the effective dispersion coefficient, z [m] is the axial dimension of the reactor, and $\mathbf{u}$ [m·s^{-1}] is the velocity.

Reducing the model to its axial dimension (z) and considering a closed-closed system (Danckwerts' boundary conditions):

$$\mathbf{u}c_0 = \mathbf{u}c|_{z=0^+} - D_a \frac{\partial c}{\partial z}\Big|_{z=0^+} \qquad \text{Eq. 6}$$

$$\frac{\partial c}{\partial z}\Big|_{z=L} = 0 \qquad \text{Eq. 7}$$

where L [m] refers to the length of the reactor.

The residence distribution of the fluid, E [s^{-1}], is obtained from the concentration of the tracer — proportional to the UV signal—normalized by the total tracer response:

$$E = \frac{c}{\int_0^t c\, dt} \qquad \text{Eq. 8}$$

The complete RTD of the system can be described by a series of convolutions:

$$E_{system} = E_{upstream} * E_{PBR} * E_{downstream} \qquad \text{Eq. 9}$$

$$E_{system} = E_{bypass} * E_{PBR} \quad \text{Eq. 10}$$

where $*$ indicates a convolution operation. Background distributions (E_{bypass}) —i.e. fittings only, no packed bed— were measured in order to convolute them using the modeled reactor. In this way, dispersion number ($\frac{D_a}{\mathbf{u}L}$) was determined by fitting the numerically solved dispersion model to experimentally measured RTDs via COMSOL MUTLIPHYSICS (v5.2a, COMSOL AB).

3. RESULTS AND DISCUSSION

To evaluate the impact of ultrasound on the hydrodynamics of the packed-beds, visualization experiments are combined with differential pressure drop measurements across the fixed bed. Abrupt and nearly instantaneous changes to the hydrodynamics induced by ultrasound are observed both qualitatively and quantitatively (Figure 2). To obtain a direct visualization of the physics of interest, additional experiments were designed using a glass tube with a concentric sonotrode resulting in a fixed bed sandwiched between the core and outer wall with a characteristic radial dimension of 1.59 mm (see SI for more details on the setup).

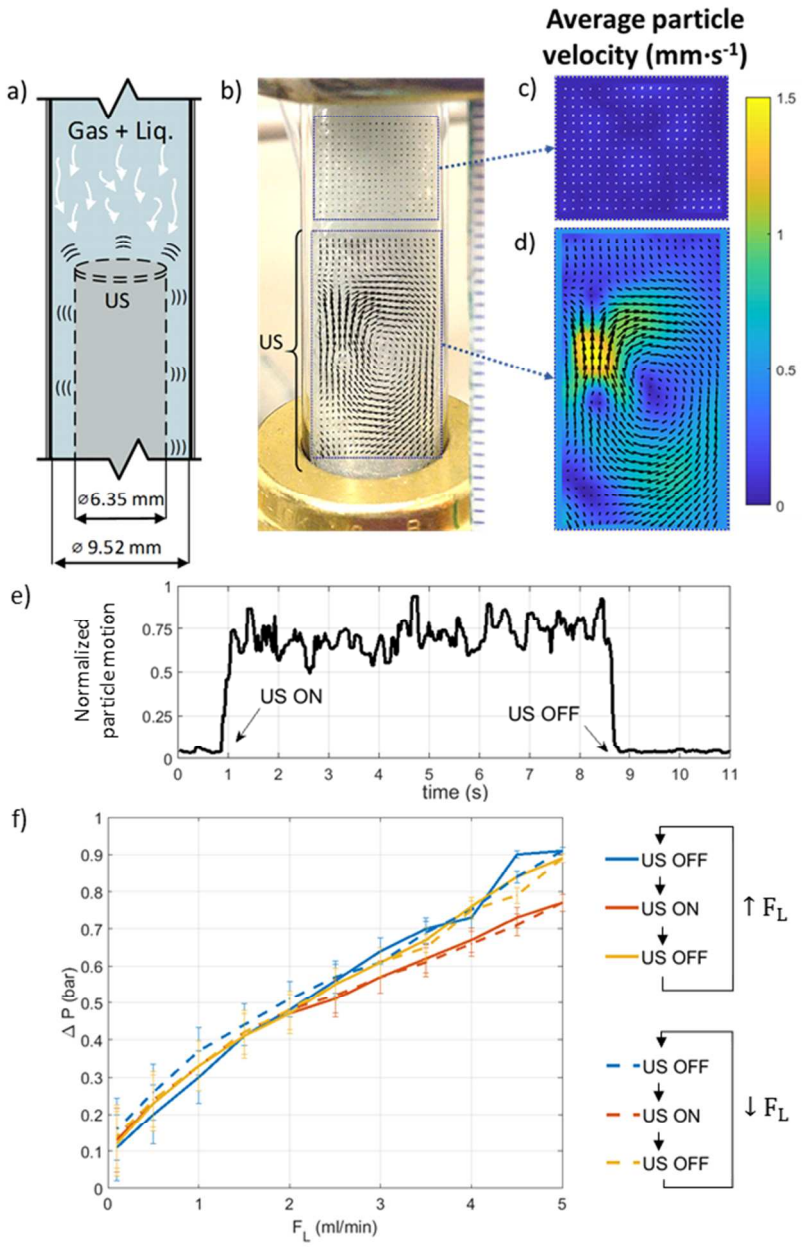

Figure 2. Partial bed fluidization of 100 µm silica glass beads packed around a sonotrode (a) resonating at ~31.8 kHz. Bed particle velocity was tracked (b) and averaged for the recorded videos in the vicinity of the sonicated area (c) and upstream were the effects were attenuated (d). The partial movement of bed particles allowed for the quantification of the response under sonicated and silent regimes using image processing algorithms (e). Corresponding decreases of pressure drop during sonication (f) reveals enhanced fluidization contributions at different liquid flow rates and constant gas flow of 100 sccm.

The packed bed in contact with the ultrasound probe (Figure 2a) shows two distinctive ultrasound induced modifications to the well-developed hydrodynamics. Specifically, partial fluidization is observed

during sonication (Supporting Video 1) as well as modification of gas-channeling (Supporting Video 2). Under sonication, the acoustic pressure and the short-range motion of particles (Figure 2b, c) continuously modifies the interstitial pore structure facilitating gas movement with a corresponding reduction in pressure drop (Figure 2f). This effect is particularly prominent at higher liquid flow rates (> 3 ml/min), where sonication induces a sudden decrease in pressure drop (5-15%). Conversely, when irradiation ceases, the pressure drop returns to the pre-sonication values indicating the enhancement is due to the dynamic reorientation of the packing material. Using the automated platform described in Figure 1, the US was irradiated from the walls of the sono-reactor with similar induced pressure drop behavior (see SI).

Next, changes in dispersion under silent and sonication conditions were assessed by RTD experiments. In the scenario where ultrasound was applied to a liquid-only flow reactor, sonication and silent distributions presented minimal differences (Figure 3a). The dispersion number increased slightly in the sonicated system (from $D_a/uL = 0.010$ to 0.013), probably due to the partial bed fluidization produced by ultrasound irradiation (Figure 3b).

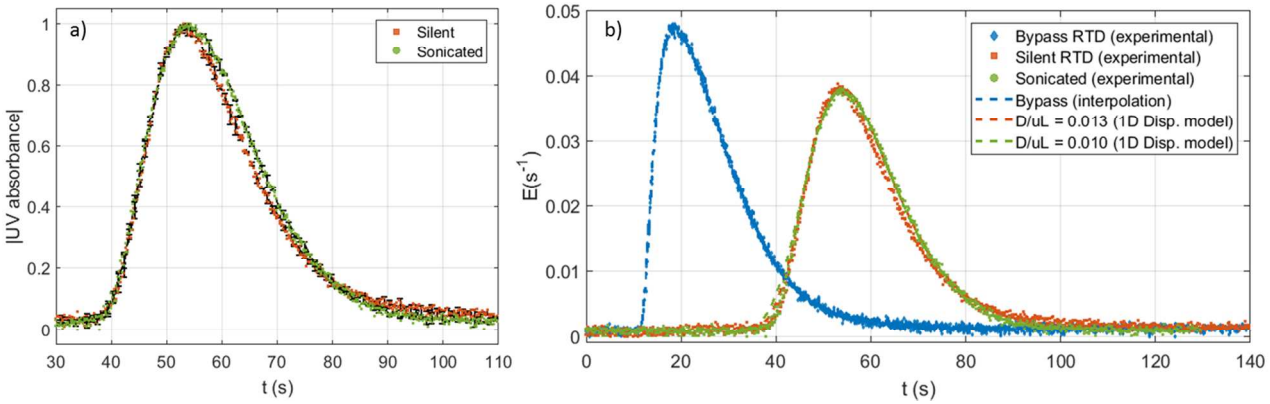

Figure 3. Normalized output signal (a) and RTD curves (b) with only liquid flowing (1 ml/min) at 38 kHz and 20 W. Sonicated and silent experiments exhibit minimal to insignificant differences in mean residence time and flow profile.

In stark contrast, the effects of ultrasound on the gas-liquid micropacked-bed reactor are significant (Figure 3). The sonicated system eludes sharply without much of the long-time tailing present in the silent experiment. Ultrasonic sonication significantly narrows the width of the RTD compared to silent conditions.

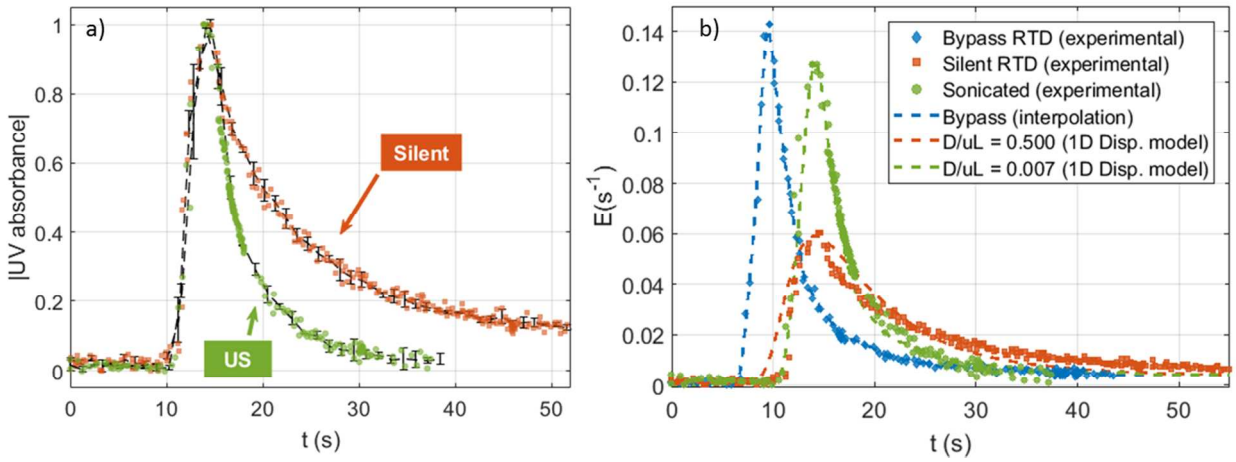

Figure 4. Normalized output signal (a) and RTD curves (b) for a two-phase flow micropacked-bed reactor. Sonicated and silent experiment results confirm significant hydrodynamic changes likely due to the reduction of gas-channeling phenomena. A simple closed-closed dispersion model is used (b) to show

how the designed US assisted PBR reduces the dispersion coefficient by nearly two orders of magnitude when compared to the silent operation.

Under silent conditions, viscous and especially capillary forces ($Ca \approx 5 \cdot 10^{-3}$) promote the formation of a segregated flow where much of the gas flows near the reactor wall. In this worst-case scenario[4], unequal velocity gradients appear radially and the tracer distributes unevenly resulting in a substantial tail in the RTD. In contrast, our study suggests through visualization experiments (Figure 2a-d and SI), that high power ultrasound can continuously modify the preferential gas channels, significantly reducing the axial dispersion (Figure 4b). This can be attributed to pore-scale phenomena occurring at the gas-liquid interface. The transmitted acoustic energy dynamically modifies the porous structure (partial fluidization) and capillary pressure, disturbing the hydrodynamic resistances and allowing eventual intercalation of the gas phase.

This drastic acoustic transformation (Figure 4b) is similar to findings recently reported in the literature where dispersion is significantly reduced in pure liquid microfluidic mixers due to vigorous liquid agitation induced, in that case, by acoustic cavitation[40]. Particularly, authors showed how the enhanced radial mixing was responsible for this reduction in dispersion.

Notably, cavitation was not observed during the visualization experiments—nor is it necessary to promote fluid movement in unconsolidated porous media[17,18]. The strong attenuation of ultrasound in porous media[32,41] suggests that any inertial cavitation will only occur in the vicinity of the radiating surfaces. A high frequency acoustic disruption of the compressible media through the bed might still be hindered by the dynamic modification of gas preferential channels. To provide some physical understanding of the dynamic forces involved, thee following dimensionless numbers are calculated to assess the vibration-induced fluid and particle motion[18] and multiphase flow in porous media[42] (Eq. 11 and 12).

$$\text{modified Bond } (Bo^*) = \frac{\text{transitional force}}{\text{capillary force}} = \frac{\rho_L a_{sonic} d_p}{\gamma/d_p} \approx 1 - 10 \quad \text{Eq. 11}$$

$$\text{Ohnesorge } (Oh) = \frac{\text{viscous force}}{\text{inertial and capillary forces}} = \frac{\mu_L}{\sqrt{\rho_L \gamma \frac{d_{confinement}}{2}}} \approx 1.5 \cdot 10^{-2} \quad \text{Eq. 12}$$

The modified Bond number expression (Eq. 12) allows qualitative evaluation of transitional acoustic forces. Instead of the gravitational force, the acceleration is estimated considering the displacement at the radiating walls —usually in the order of 10 μm for ultrasonic cleaning transducers[27]— and the applied frequency. The result of this estimation ($Bo^* \approx 1 - 10$) provides some insights regarding how a well-designed power-ultrasound reactor can offset capillary forces in micropacked-bed geometries. Finally, analyzing the Ohnesorge number (Eq. 12), some bubble break-up can be expected[42] within the interstitial constrictions between particles as Oh <0.01. Therefore, if the vibrations produced by sonication can slightly alter the interparticle geometry or the gas-liquid interphase as suggested by the modified Bond number, an increase of break-up of bubbles should be expected. Combined with our experimental pressure drop, fluidization regime change, and decreased dispersion findings, these dimensionless analyses suggest that ultrasonication of packed beds may induce minor bed vibrations capable of overcoming capillary and viscous forces to induce bubble break-up and bed homogenization.

4. CONCLUSIONS

We have shown how ultrasound reduces dispersion in micropacked-bed reactors by two orders of magnitude. Sonication produces partial fluidization of the bed even at high flow rates, continuously modifying gas channels and reducing liquid dispersion. Direct visualization and RTD experiments confirm that ultrasound can remove common gas channeling phenomena by promoting a dynamically dispersed gas phase flow. A more thorough study under a variety of hydrodynamics conditions is still necessary to assess contributions to mass transfer, the nature of gas-channeling and the potential for enhancing heterogeneous catalyst reactions. The effects of short ultrasound pulses applied during transient initial

bed operation might also present an interesting area of exploration to reduce variation in bed packing and ensure a more uniform packing for longer runtimes. To mitigate any surface damage of the catalyst due to cavitation or friction, more data are essential to quantify the acoustic attenuation in unsaturated porous media and to optimize the design of micropacked-bed sonoreactors. The efficient use of ultrasound unlocks new pathways for multiphase reactor design and use, enabling near-plug-flow operation with enhanced phase homogenization in micro-scale packed beds.

5. ACKNOWLEDGEMENTS

This research was partially funded by the EU project MAPSYN: Microwave, Acoustic and Plasma SYNtheses, under grant agreement No. CP-IP 309376 of the European Union Seventh Framework Program. The support of the Novartis-MIT Centre for Continuous Manufacturing is acknowledged. Authors would like to thank P. Poveda and Prof. J. Ramis (University of Alicante) for the electro-mechanical characterization of the designed sonoreactor.

SUPPORTING INFORMATION

RTD experimental setup and design; visualization setup and image analysis methodology; raw and processed flow, pressure and temperature data for silent and sonicated flow experiments; sonotrode design methodology and characterization; experimental assessment of ultrasound-induced particle attrition; supporting videos of bed fluidization and gas channeling.

AUTHOR INFORMATION

Corresponding Author

*(Klavs F. Jensen) E-mail: kfjensen@mit.edu

ORCID

Francisco J. Navarro-Brull: 0000-0001-7482-9485

Andrew R. Teixeira: 0000-0003-2889-9102

Jisong Zhang: 0000-0001-7940-6860

Roberto Gómez: 0000-0002-5231-8032

Klavs F. Jensen: 0000-0001-7192-580X

Notes

The authors declare no competing financial interest.

6. REFERENCES

(1) van Herk, D.; Kreutzer, M. T.; Makkee, M.; Moulijn, J. A. Scaling down Trickle Bed Reactors. *Catal. Today* **2005**, *106*, 227–232.

(2) van Herk, D.; Castaño, P.; Makkee, M.; Moulijn, J. A.; Kreutzer, M. T. Catalyst Testing in a Multiple-Parallel, Gas–liquid, Powder-Packed Bed Microreactor. *Appl. Catal. Gen.* **2009**, *365*, 199–206.

(3) Bryan, M. C.; Wernick, D.; Hein, C. D.; Petersen, J. V.; Eschelbach, J. W.; Doherty, E. M. Evaluation of a Commercial Packed Bed Flow Hydrogenator for Reaction Screening, Optimization, and Synthesis. *Beilstein J. Org. Chem.* **2011**, *7*, 1141–1149.

(4) Moulijn, J. A.; Makkee, M.; Berger, R. J. Catalyst Testing in Multiphase Micro-Packed-Bed Reactors; Criterion for Radial Mass Transport. *Catal. Today* **2016**, *259*, 354–359.

(5) Faridkhou, A.; Tourvieille, J.-N.; Larachi, F. Reactions, Hydrodynamics and Mass Transfer in Micro-Packed Beds—Overview and New Mass Transfer Data. *Chem. Eng. Process. Process Intensif.* **2016**, *110*, 80–96.

(6) Márquez, N.; Castaño, P.; Makkee, M.; Moulijn, J. A.; Kreutzer, M. T. Dispersion and Holdup in Multiphase Packed Bed Microreactors. *Chem. Eng. Technol.* **2008**, *31*, 1130–1139.

(7) Iliuta, I.; Hamidipour, M.; Schweich, D.; Larachi, F. Two-Phase Flow in Packed-Bed Microreactors: Experiments, Model and Simulations. *Chem. Eng. Sci.* **2012**, *73*, 299–313.

(8) Alsolami, B. H.; Berger, R. J.; Makkee, M.; Moulijn, J. A. Catalyst Performance Testing in Multiphase Systems: Implications of Using Small Catalyst Particles in Hydrodesulfurization. *Ind. Eng. Chem. Res.* **2013**, *52*, 9069–9085.

(9) Lenormand, R.; Touboul, E.; Zarcone, C. Numerical Models and Experiments on Immiscible Displacements in Porous Media. *J. Fluid Mech.* **1988**, *189*, 165–187.

(10) Trojer, M.; Szulczewski, M. L.; Juanes, R. Stabilizing Fluid-Fluid Displacements in Porous Media Through Wettability Alteration. *Phys. Rev. Appl.* **2015**, *3*, 054008.

(11) Zhao, B.; MacMinn, C. W.; Juanes, R. Wettability Control on Multiphase Flow in Patterned Microfluidics. *Proc. Natl. Acad. Sci.* **2016**, *113*, 10251–10256.

(12) Holtzman, R. Effects of Pore-Scale Disorder on Fluid Displacement in Partially-Wettable Porous Media. *Sci. Rep.* **2016**, *6*, srep36221.

(13) Lo, W.-C.; Yang, C.-C.; Hsu, S.-Y.; Chen, C.-H.; Yeh, C.-L.; Hilpert, M. The Dynamic Response of the Water Retention Curve in Unsaturated Soils during Drainage to Acoustic Excitations. *Water Resour. Res.* **2017**, *53*, 712–725.

(14) Beresnev, I.; Gaul, W.; Vigil, R. D. Direct Pore-level Observation of Permeability Increase in Two-phase Flow by Shaking. *Geophys. Res. Lett.* **2011**, L20302.

(15) Manga, M.; Beresnev, I.; Brodsky, E. E.; Elkhoury, J. E.; Elsworth, D.; Ingebritsen, S. E.; Mays, D. C.; Wang, C.-Y. Changes in Permeability Caused by Transient Stresses: Field Observations, Experiments, and Mechanisms. *Rev. Geophys.* **2012**, *50*, RG2004.

(16) Müller, T. M.; Caspari, E.; Qi, Q.; Rubino, J. G.; Velis, D.; Lopes, S.; Lebedev, M.; Gurevich, B. Chapter 3 - Acoustics of Partially Saturated Rocks: Theory and Experiments. In *Seismic Exploration of Hydrocarbons in Heterogeneous Reservoirs*; Elsevier, 2015.

(17) Stewart, R. A.; Shaw, J. M. A Dynamic Pressure View Cell for Acoustic Stimulation of Fluids—Micro-Bubble Generation and Fluid Movement in Porous Media. *Rev. Sci. Instrum.* **2015**, *86*, 095101.

(18) Stewart, R. A.; Shaw, J. M. On Vibration-Induced Fluid and Particle Motion in Unconsolidated Porous Media: Observations and Dimensional Scaling Analysis. *Transp. Porous Media* **2017**, *116*, 1031–1055.

(19) Naderi, K.; Babadagli, T. Visual Analysis of Immiscible Displacement Processes in Porous Media under Ultrasound Effect. *Phys. Rev. E* **2011**, *83*, 056323.

(20) Keshavarzi, B.; Karimi, R.; Najafi, I.; Ghotbi, C.; Ghazanfari, M. H. Investigating the Role of Ultrasonic Wave on Two-Phase Relative Permeability in Free Gravity Drainage Process. *Sci. Iran.* **2014**, *21*, 763–771.

(21) Rivas, D. F.; Cintas, P.; Gardeniers, H. J. G. E. Merging Microfluidics and Sonochemistry: Towards Greener and More Efficient Micro-Sono-Reactors. *Chem. Commun.* **2012**, *48*, 10935–10947.

(22) Rivas, D. F.; Kuhn, S. Synergy of Microfluidics and Ultrasound. *Top. Curr. Chem.* **2016**, *374*, 70.

(23) Rossi, D.; Jamshidi, R.; Saffari, N.; Kuhn, S.; Gavriilidis, A.; Mazzei, L. Continuous-Flow Sonocrystallization in Droplet-Based Microfluidics. *Cryst. Growth Des.* **2015**, *15*, 5519–5529.

(24) Dong, Z.; Yao, C.; Zhang, X.; Xu, J.; Chen, G.; Zhao, Y.; Yuan, Q. A High-Power Ultrasonic Microreactor and Its Application in Gas–liquid Mass Transfer Intensification. *Lab. Chip* **2015**, *15*, 1145–1152.

(25) John, J. J.; Kuhn, S.; Braeken, L.; Van Gerven, T. Ultrasound Assisted Liquid–liquid Extraction with a Novel Interval-Contact Reactor. *Chem. Eng. Process. Process Intensif.* **2017**, *113*, 35–41.

(26) Tandiono; Ohl, S.-W.; Ow, D. S.-W.; Klaseboer, E.; Wong, V. V. T.; Camattari, A.; Ohl, C.-D. Creation of Cavitation Activity in a Microfluidic Device through Acoustically Driven Capillary Waves. *Lab Chip* **2010**, *10*, 1848–1855.

(27) Mason, T. J.; Lorimer, J. P. General Principles. In *Applied Sonochemistry: Uses of Power Ultrasound in Chemistry and Processing*; Wiley-VCH Verlag GmbH & Co. KGaA, **2002**.

(28) Tudela, I.; Sáez, V.; Esclapez, M. D.; Díez-García, M. I.; Bonete, P.; González-García, J. Simulation of the Spatial Distribution of the Acoustic Pressure in Sonochemical Reactors with Numerical Methods: A Review. *Ultrason. Sonochem.* **2014**, *21*, 909–919.

(29) Navarro-Brull, F.J.; Poveda, P.; Ruiz-Femenia, R.; Bonete, P.; Ramis, J.; Gómez, R. Guidelines for the Design of Efficient Sono-Microreactors. *Green Process. Synth.* **2014**, *3*, 311.

(30) Peshkovsky, S. L.; Peshkovsky, A. S. Matching a Transducer to Water at Cavitation: Acoustic Horn Design Principles. *Ultrason. Sonochem.* **2007**, *14*, 314–322.

(31) Bouzidi, Y.; Schmitt, D. R. Measurement of the Speed and Attenuation of the Biot Slow Wave Using a Large Ultrasonic Transmitter. *J. Geophys. Res. Solid Earth* **2009**, *114*, B08201.

(32) Sessarego, J. P.; Guillermin, R. High-Frequency Sound-Speed, Attenuation, and Reflection Measurements Using Water-Saturated Glass Beads of Different Sizes. *IEEE J. Ocean. Eng.* **2012**, *37*, 507–515.

(33) Serpieri, R.; Corte, A. D.; Travascio, F.; Rosati, L. Variational Theories of Two-Phase Continuum Poroelastic Mixtures: A Short Survey. In *Generalized Continua as Models for Classical and Advanced Materials*; Advanced Structured Materials; Springer, Cham, **2016**.

(34) John, J. J.; Kuhn, S.; Braeken, L.; Van Gerven, T. Temperature Controlled Interval Contact Design for Ultrasound Assisted Liquid–liquid Extraction. *Chem. Eng. Res. Des.* **2017**, *125*, 146–155.
(35) Zhang, J.; Teixeira, A. R.; Kögl, L. T.; Yang, L.; Jensen, K. F. Hydrodynamics of Gas–liquid Flow in Micropacked Beds: Pressure Drop, Liquid Holdup, and Two-Phase Model. *AIChE J.* **2017**, *63*, 4694–4704.
(36) Zhang, J.; Teixeira, A. R.; Jensen, K. F. Automated Measurements of Gas-Liquid Mass Transfer in Micropacked Bed Reactors. *AIChE J. In Press*, 10.1002/aic.15941.
(37) Adamo, A.; Heider, P. L.; Weeranoppanant, N.; Jensen, K. F. Membrane-Based, Liquid–Liquid Separator with Integrated Pressure Control. *Ind. Eng. Chem. Res.* **2013**, *52*, 10802–10808.
(38) Thielicke, W.; Stamhuis, E. PIVlab – Towards User-Friendly, Affordable and Accurate Digital Particle Image Velocimetry in MATLAB. *J. Open Res. Softw.* **2014**, *2*, e30.
(39) Fogler, H. S. *Elements of Chemical Reaction Engineering*; Elements of Chemical Reaction Engineering; Prentice Hall PTR, **2006**.
(40) Dong, Z.; Zhao, S.; Zhang, Y.; Yao, C.; Yuan, Q.; Chen, G. Mixing and Residence Time Distribution in Ultrasonic Microreactors. *AIChE J.* **2017**, *63*, 1404–1418.
(41) Lesnik, S.; Mettin, R.; Brenner, G. Study of Ultrasound Propagation and Cavitation Activity in a Packing Bed of Spherical Particles. *Chem. Ing. Tech.* **2017**, *89*, 1379–1384.
(42) Olbricht, W. L. Pore-Scale Prototypes of Multiphase Flow in Porous Media. *Annu. Rev. Fluid Mech.* **1996**, *28*, 187–213.

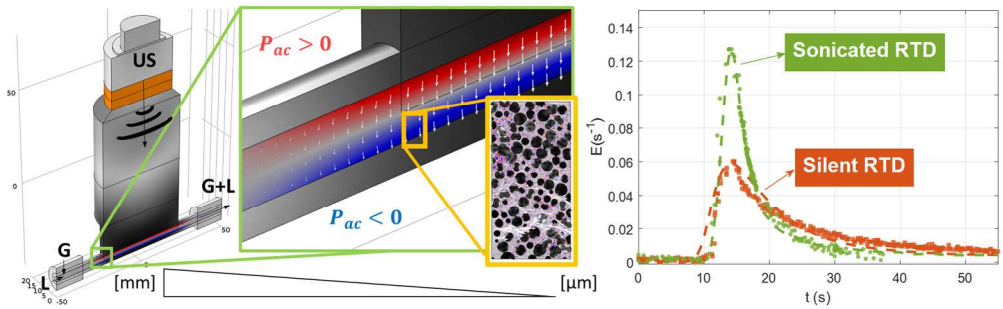

TOC graphic

519x158mm (96 x 96 DPI)